Available online at www.sciencedirect.com
SCIENCE DIRECT
Biosensors and Bioelectronics 21 (2006) 1924–1931
BIOSENSORS & BIOELECTRONICS
www.elsevier.com/locate/bios

Highly sensitive revealing of PCR products with capillary electrophoresis based on single photon detection

Evgeni A. Kabotyanski [a,*], Inna L. Botchkina [b], Olga Kosobokova [a], Galina I. Botchkina [b], Vera Gorfinkel [a], Boris Gorbovitski [c]

[a] *Department of Electrical and Computer Engineering, State University of New York at Stony Brook, Stony Brook, NY 11794, USA*
[b] *Department of Surgery and Surgical Oncology, State University of New York at Stony Brook, Stony Brook, NY 11794, USA*
[c] *BioPhotonics Corporation, Stony Brook, NY 11794, USA*

Received 29 August 2005; received in revised form 1 December 2005; accepted 4 January 2006
Available online 3 March 2006

Abstract

Post-PCR fragment analysis was conducted using our single photon detection-based DNA sequencing instrument in order to substantially enhance the detection of nucleic biomarkers. Telomerase Repeat Amplification Protocol assay was used as a model for real-time PCR-based amplification and detection of DNA. Using TRAPeze XL kit, telomerase-extended DNA fragments were obtained in extracts of serial 10-fold dilutions of telomerase-positive cells, then amplified and detected during 40-cycle real-time PCR. Subsequently, characteristic 6-base DNA ladder patterns were revealed in the post-PCR samples with capillary electrophoresis (CE). In our CE instrument, fluorescently labeled DNA fragments separate in a single-capillary module and are illuminated by a fiberized Ar-ion laser. The laser-induced fluorescence (LIF) is filtered and detected by the fiberized single photon detector (SPD). To assess the sensitivity of our instrument, we performed PCR at fewer cycles (29 and 25), so that the PCR machine could detect amplification only in the most concentrated samples, and then examined samples with CE. Indeed, PCR has detected amplification in samples with minimum 10^4 cells at 29 cycles and over 10^5 cells at 25 cycles. In contrast, the SPD-based CE–LIF has revealed 6-base repeats in samples with as low as 10^2 cells after 29 cycles and 10^3 cells after 25 cycles. Thus, we have demonstrated 100- to 1000-fold increase in the sensitivity of biomarker detection over real-time PCR, making our approach especially suitable for analysis of clinical samples where abundant PCR inhibitors often cause false-negative results.

Keywords: Real-time PCR; Capillary electrophoresis; Single photon detection; Laser-induced fluorescence; Telomerase activity; TRAP

1. Introduction

Utmost sensitivity and verifiability in detecting molecular markers are critical but still limiting factors in advancing molecular diagnostics of cancer to point-of-care. PCR-based methods can detect biomarkers of the most common malignancies in much fewer cells than conventional histological or cytological examination. Moreover, methods based on real-time PCR exhibit highest sensitivity and range, along with a degree of quantization, which makes real-time PCR the most promising basis for the development of molecular methods of cancer detection (e.g., de Kok et al., 2000). The diagnostic value of a particular real-time PCR method depends on the fluorescent reporter chemistry being used. Non-specific reporters, such as SYBR Green, provide the highest degree of sensitivity, but with a high incidence of non-specific amplification and false-positive results. Use of specific probes, e.g., Molecular Beacons, Scorpions, Amplifluors, etc., ensures higher specificity, but it comes at the expense of sensitivity and thus produces a high rate of false-negative results.

Therefore, sensitivity of PCR and its careful validation are critical, especially for real clinical samples. Although several commercial PCR-based assays already claim single cell/single copy sensitivity, the claims are based on experiments with clean tumor cell lines and pure PCR reagents, when PCR efficiency is very high (1.8–1.9). Yet single cell/copy samples become detectable only at very late cycles (40–45). In clinical conditions, however, low levels of input material are amplified in the presence of various inhibitors of the Taq polymerase, as well as nucleases, proteases, or other suppressors collected along

* Corresponding author.
E-mail address: eak@dnalab.cc (E.A. Kabotyanski).

0956-5663/$ – see front matter © 2006 Elsevier B.V. All rights reserved.
doi:10.1016/j.bios.2006.01.015

with specimens. This makes the efficiency of PCR in clinical samples much lower than in ideal test samples. For example, several studies evaluating standard assays for telomerase activity showed that the number of cells required for tumor detection varied from 250 to 5000 cells (Wu et al., 2000b). Obviously, in clinical samples containing inhibitors, a low level of the target may well become undetectable at all. Therefore, a significant (2–3 orders of magnitude) increase in the sensitivity, along with a simple method of validation of PCR outcome, is needed for PCR to become a reliable tool in patient care.

The main factor limiting sensitivity of real-time PCR is high background fluorescence of probes that are not bound to the PCR product. Separating DNA fragments with capillary electrophoresis (CE) and detecting their laser-induced fluorescence (LIF) eliminates the background fluorescence, allows concentration of the PCR product due to the sample stacking during the electrokinetic injection, and thus improves sensitivity (e.g., Schwartz and Ulfelder, 1992). To further lower the detection threshold, we combined CE–LIF with single photon detector (SPD). Sensitivity of SPDs is intrinsically very high due to their very high quantum yield and extremely low dark count. In addition, the electric output of an SPD can be directly processed by a digital circuitry. Hence signal amplification, recording and processing steps do not add any noise to the detected signal as opposed to common LIF systems. The only unavoidable noise in an SPD is the stochastic noise of the measured photon flux (Alaverdian et al., 2002). We expected that a CE–LIF–SPD system would have sensitivity several orders of magnitude higher than that of real-time PCR. As a concept-proving step, we conducted post-PCR fragment analysis with our CE–LIF–SPD instrument in order to assess the degree to which it enhances the detection of molecular biomarkers. The analysis of *telomerase* was used as a very important and relevant model.

Of about a hundred of discovered cancer-related molecular markers, telomerase is considered the most promising one. Functional telomerase is present in about 90% of all human cancers, but, in contrast, it is generally absent from most benign tumors and normal somatic (except germ line and stem) cells (Kim et al., 1994; Shay and Wright, 1996). The detection of telomerase activity has the highest combination of sensitivity (60–90%) and clinical specificity (94–100%) when compared to other screening methods (Hess and Highsmith, 2002; Hiyama and Hiyama, 2002). The activity of telomerase has been proven as the most accurate marker for cancer detection, staging and prognosis (Dhaene et al., 2000).

The ends of chromosomes consist of thousands of double-stranded (ds) TTAGGG repeats called *telomeres* that have several functions (Blackburn, 1991). In normal somatic cells, telomere length is progressively shortened with each cell division, eventually leading to cell death. In contrast, unlimited proliferation of most immortal and cancer cells is highly dependent on the activity of telomerase, which compensates for replicate telomere losses by elongating existing telomere with TTAGGG repeats, using its own RNA component as a template (Blackburn, 1991).

Currently, the detection of telomerase activity is based on the telomeric repeat amplification protocol (TRAP), which employs the ability of telomerase to recognize and elongate in vitro an artificial oligonucleotide substrate, TS, and then uses PCR to amplify the extended DNA products (Kim et al., 1994). A significant improvement of the assay is the real-time quantitative TRAP (RTQ-TRAP) (Hou et al., 2001), which combines the conventional TRAP assay and a real-time PCR based on SYBR Green. More specific telomerase detection was also demonstrated with HEX-labeled TS primer (Atha et al., 2003), as well as using TRAPeze XL kit that employs Amplifluor primers (Elmore et al., 2002). Utilization of labeled primers has the added advantage of enabling fast and simple verification and quantitation of telomerase with CE–LIF (Hess et al., 2004; Jakupciak et al., 2004).

In the present study, we have demonstrated for the first time the use of the TRAPeze XL kit for both real-time PCR amplification and CE–LIF detection of telomeric repeats. In post-PCR fragment analysis with our SPD-based DNA sequencer, we have demonstrated a 100- to 1000-fold increase in the sensitivity of telomerase detection compared to the sensitivity of the real-time PCR method. Preliminary results of this work were reported elsewhere (Kabotyanski et al., 2005).

2. Materials and methods

2.1. DNA sequencer

SPD-based DNA sequencer was developed earlier in our group (Alaverdian et al., 2002). DNA samples undergo separation in a single-capillary separation module comprised of a miniature high voltage supply (up to 15 kV) with a built-in voltmeter and amperemeter, a polymer replacement system, a temperature control system (25–70 ± 0.01 °C), a tube-changer carousel for DNA samples and running buffer, and a precision optical system. When the fluorescently labeled DNA fragments pass the optical system, they are illuminated by a fiberized Ar-ion laser (488 and 514 nm, 20 mW, Uniphase, CA, USA). The LIF is filtered and detected by the fiberized avalanche photo diode-based SPD (SPCM-AQ4C, Perkin-Elmer, CA, USA). A photon counting circuit board based on field programmed gate array (FPGA) technology is used to count, integrate, and transfer the data to a computer.

2.2. PCR assays

RTQ-TRAP was performed in a 96-well plate format using DNA Engine Opticon (MJ Research, MA). QuantiTect SYBR Green PCR kit (Qiagen, CA) and TRAPeze XL telomerase detection kit (Chemicon, CA) were used according to manufacturers' instructions with some modifications.

2.2.1. Protein extracts from telomerase-positive cells

One source of telomerase was the control cell pellet (10^6 telomerase-positive cells) provided with the TRAPeze XL telomerase detection kit (Chemicon, CA). Alternatively, 10^6 cells pellets of PC-3 cells (provided by the Cell Culture/Hybridoma facility, SUNY Stony Brook, NY) were used. Cells pellets were resuspended in ice-cold CHAPS lysis buffer

containing 100 U/ml of SUPERase (Ambion), incubated on ice for 30 min, and centrifuged (16,000 × *g*, 20 min, 4 °C). The supernatant was removed, aliquoted, serially diluted 1:10 in CHAPS lysis buffer (10^6–10 cell extracts per 20 μl), snap frozen and stored at −80 °C. 2 μl of an aliquot were further used for RTQ-TRAP (final dilutions were 10^5–1 cells).

2.2.2. Telomerase extension

Reaction mixtures of either kit (25 μl/well) were first incubated at 25 °C for 30 min to allow the telomerase in the extract to elongate the TS primer. The extension reaction products, DNA molecules with telomeric repeats in 6-base increments, served as templates for the following PCR. In some experiments, TSR8 control template DNA (Chemicon) in final concentrations of 0.02 and 0.002 amoles/μl was used as positive control. Reaction mixture without cell extract was used as a negative control. Samples were examined in duplicates or triplicates.

2.2.3. QuantiTect kit

Primers: Telomerase substrate and forward, TS: 5′-AATCCGTCGAGCAGAGTT-3′; reverse, ACX: 5′-GCGCGGCTTACCCTTACCCTTACCCTAACC-3′ (Invitrogen, CA) were added to reaction mix prior extension at 0.2 μM. Cycling: 95 °C for 15 min (hot start), followed by 40-cycle amplification (denaturation at 95 °C for 30 s; annealing at 55 °C for 30 s; extension for 60 s and plate reading for 10 s at 72 °C), and 4 °C hold. In some experiments the melting curve was read from 65 to 95 °C.

2.2.4. TRAPeze XL kit

Primers: The working of the Amplifluor primers is well explained in the manual (http://www.chemicon.com/webfiles/PDF/S7707.pdf) and in Elmore et al. (2002). The reaction mixture already contains TS forward and fluorescein-labeled Amplifluor RP reverse primers generating green fluorescing products. It also contains a sulforhodamine-labeled Amplifluor K2 reverse primer for the semi-competitive simultaneous amplification of the internal control template TSK2 generating a red-fluorescent 56-base product. Wild type (FastStart by Roche, IN) or Titanium (Clontech, CA) Taq DNA polymerases were also added to the reaction mix at 0.5 μl (~2.5 wild type Units) prior extension. Cycling: 95 °C for 1 min (hot start), followed by 40-cycle amplification (denaturation at 94 °C for 30 s; annealing at 55 °C for 30 s; extension for 60 s and plate reading for 5 s at 68 °C), 3 min incubation at 68 °C, and 4 °C hold. In some experiments the melting curve was read from 65 to 95 °C after final 3 min incubation at 55 °C.

2.3. CE

Polyimide coated fused silica capillary tubing (TSP050375, Polymicro, AZ), 50 μm i.d., was used. LIF was detected at 50 cm, where 1 cm of coating was removed by heat.

2.3.1. CE in non-denaturing gel

PCR products labeled by SYBR Green I with QuantiTect kit were separated in non-denaturing Genescan Polymer (GSP) (Applied Biosystems, CA), 5% in ABI buffer. Samples were diluted 1:5 in ultra pure H_2O, then electrokinetically injected (25 s, 10 kV) and separated at 8 kV at 25 °C.

2.3.2. CE in denaturing gel

Fluorescein-labeled PCR products obtained with TRAPeze XL kit were separated in denaturing POP-7 gel (Applied Biosystems). Samples were usually used without clean-up, but in some experiments they were first de-salted with Performa spin-columns (Edge BioSystems, MD) by spinning 2 min at 750 × *g*. Preparation of samples for CE: (1) mixing 1 μl of PCR product with 9 μl Hi-Di formamide (Applied Biosystems), heating the mixture for 3 min at 94 °C and flash-chilling on ice; or (2) mixing 2 μl of PCR product with 2 μl Hi-Di formamide, heating the mixture for 3 min at 94 °C and flash-chilling on ice, then mixing it with 16 μl of ice-cold ultra pure H_2O. Electrokinetic injection: usually at 5 kV for 40 s. Separation: at 8 kV at 50 °C. In some instances, 0.5 μl of Internal Lane Standard 600 (ILS) (Promega, CA) was added to a sample for size scaling.

2.4. Data processing and analysis

Data were collected and analyzed using our software, which includes separate modules for run data recording (MONITOR), processing, visualization, and editing (BASE). The MONITOR accepts the sampled fluorescence data via the Parallel Port, performs real-time visualization and recording to a 'raw' on the hard drive. The BASE produces fully processed *PHRED*-compatible data files and provides a visual interface for viewing, manual processing, editing and printing of 'raw' and processed data.

3. Results

3.1. SYBR Green-labeled PCR products

3.1.1. PCR

Using QuantiTect kit, we obtained amplification curves for serial 10-fold dilutions of extracts of telomerase-positive cells (10^5–0.1 cells) (Fig. 1). The data were similar to those obtained previously in our group (Botchkina et al., 2005) or by others (Wege et al., 2003). These experiments also demonstrated that the assay had a limited linearity: there was some inhibition at

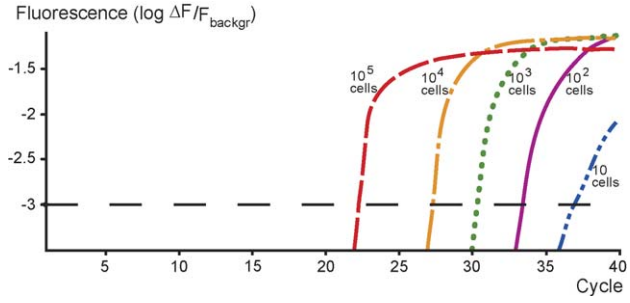

Fig. 1. Real-time PCR with QuantiTect kit. SYBR Green fluorescence values (in logarithmic scale) were obtained from wells containing serial dilutions of cell extracts (from left, 10^5–0.1 cells) and plotted against cycle numbers. Rightmost curve for 10 cells (double chain blue) reveals distinct kinetics. The 1 and 0.1 cell and negative control had 0 values (not shown). Horizontal dashed line, Ct threshold.

high concentrations (10^5 cells – left-most, dashed red curve), while at lower than 100 cell concentrations there was either no amplification (1 and 0.1 cell) or the kinetics were such that they suggested a false-positive result (10 cells – right-most, double chain blue curve). Accordingly, in the subsequent experiments we used only five dilutions from 10^5 to 10.

3.1.2. CE–LIF–SPD

After PCR, fragment analysis in a denaturing gel (POP 7) predictably gave negative results, because SYBR Green is non-covalently bonded to dsDNA. Fluorescent material was detected only with non-denaturing GSP gel. Only pherograms of the samples with the highest concentrations (10^5 and 10^4 cells) were distinguishable from those of negative controls and appeared as DNA repeats ladder. Thus, CE–LIF–SPD of material obtained with SYBR-based chemistry does not exhibit any benefits over PCR.

3.2. Covalently labeled PCR products

3.2.1. Optimization of real-time PCR with TRAPeze XL

We next used TRAPeze XL kit that employed covalently labeled primers. The kit was not specifically designed for real-time PCR, so we optimized the protocol. First we compared widely used wild type and Titanium Taq polymerases. The latter is a mutant with increased solubility and the loss of the 5′-exonuclease activity. Using cycling parameters for QuantiTect kit, we have found that Titanium resulted in higher PCR efficiency and/or increased sensitivity, as manifested by steeper amplification slopes and lower Ct values (data not shown here).

Cycling temperatures appeared to be critical for real-time detection of fluorescence. Unlike with SYBR Green, where maximal signal fluorescence exceeds background fluorescence ($\Delta F/F_{backgr}$) by ∼100%, with Amplifluor chemistry maximal fluorescence exceeded background by ∼40% at plate read temperature of 72 °C. Measuring melting curves revealed that as temperature increased, fluorescence changed differently in different concentration of PCR product. In negative control or low abundance samples, background fluorescence was low at 65 °C and slightly increased toward 80–85 °C, whereas in wells with abundant amplicons the fluorescence was maximal at 65 °C and then greatly decreased to background level at 80–85 °C (Fig. 2, insert). Thus, the signal to background ratio was better at lower temperatures. Therefore, we had decreased plate reading temperature and the temperature of the preceding extension step to 68 °C, which is lower optimum range of Titanium Taq. Consequently, maximal signal had increased to exceed background by ∼60%.

3.2.2. PCR

Our results confirmed that TRAPeze XL can be used in the real-time PCR (Fig. 2). The sensitivity of this kit was very similar to that of QuantiTect, based on Ct values for same dilutions. The important difference was that for 10 cells extracts, there was no amplification detected, which additionally indicated that in QuantiTect kit, amplification in 10 cells samples was false-positive. Because of very high specificity of TRAPeze XL, lack

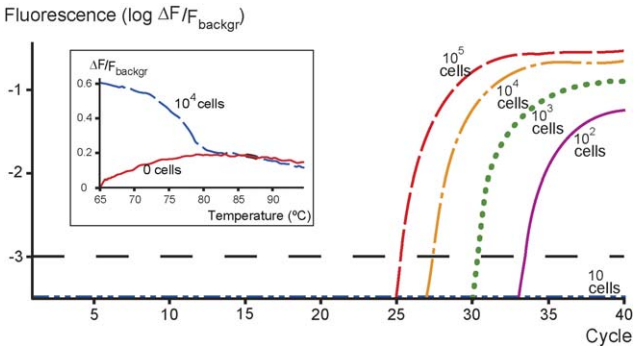

Fig. 2. Real-time PCR amplification with TRAPeze XL kit. Semi-log plot of amplification curves obtained from serial cell extracts dilutions (from left, 10^5–10^2 cells). The 10 cell extract exhibited no amplification—bottom line, double chain blue. Horizontal dashed line, Ct threshold. ***Insert***: melting curves (relative intensities) recorded after PCR from wells with negative control (lower, solid red) and 10^4 cells extract (upper, dashed blue); their dynamics are reverse and differences diminish with the increase of temperature.

of amplification in 10 cells extracts appeared to be true negative. However, because 10 cells may contain 1–5 active telomerases (Meid et al., 2001), this result needed further validation with CE–LIF–SPD.

Ct values for 10^5 cells were 25–26 cycles (median 25); for 10^4 cells, 27–29 (median 28); for 10^3 cells, 29–31 (median 30) and for 10^2 cells, 32–36 (median 34). The slopes of amplification at semi-log linear phase (Fig. 2) were not as steep as with QuantiTect (Fig. 1). This indicated somewhat slower kinetics of PCR with TRAPeze, which in part could be explained by a competition from internal control templates for the TS primer. In addition, unlike with the QuantiTect, fluorescence at the saturation phase was proportional to initial concentration. This is explained by the undisclosed design of TRAPeze XL originally intended for end point PCR quantitation.

3.2.3. CE–LIF–SPD analysis

After PCR, samples were subjected to fragment analysis. Since our instrument detected in four color bands (546 ± 5, 560 ± 5, 590 ± 5, and 610 ± 5 nm wavelengths with barrier filter 540 ± 5 nm), we used color deconvolution to image red-labeled control DNA and green-labeled telomerase-extended repeats. For the red color, a transfer matrix was obtained from the peak corresponding to sulforhodamine-labeled internal control amplicons in electropherograms of negative control samples. For the green color, we used 10^3 cells samples; the matrix was taken from one of the peaks corresponding to green fluorescing telomerase-extended DNA. Co-injection with the ILS calibration ladder proved that the large red peak corresponded to 56 bases, whereas the green peaks were six bases apart and corresponded to 55, 61, 67, etc., bases (Fig. 3). This matched the sizes of the control template and telomere repeats ladder expected from the kit manual, except for the 55-base peak not mentioned there.

3.2.4. Optimization of CE-LIF-SPD

We omitted post-PCR clean-up for simplicity of the protocol and obtained good results because only specifically labeled products were detected. However, desalting samples with Per-

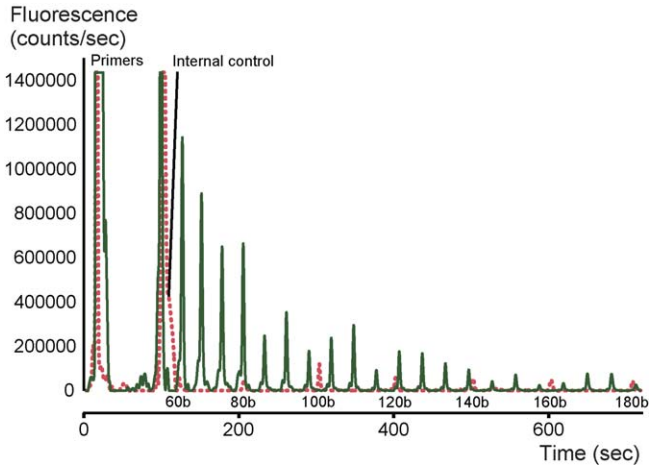

Fig. 3. Color-deconvoluted, baseline removed, electropherogram of 10^2 cells sample co-injected with ILS after real-time PCR with TRAPeze (optimized injection). Red-fluorescing materials (control template and ILS) are depicted by dotted red trace, green fluorescing – by solid green trace. Small dotted red peaks are ILS' 60, 80, 100, etc., base marks, as indicated. Telomerase-extended DNA repeats appear as peaks on the solid green trace.

forma spin columns resulted in two to three times increase in peak amplitude (not shown here).

Initially samples were prepared for CE as widely done in the field: diluting post-PCR solution in formamide 1:10 and denaturing before electrokinetic injection. Results were satisfactory. However, since formamide is hundreds of times more ionized than ultra pure H_2O, we modified sample preparation so that injection medium was less ionized and thus favored electrokinesis of DNA. We first denatured and stabilized DNA in a smaller amount of formamide (1:1), and then further diluted it 1:5 in ultra pure H_2O (see Section 2). This protocol further improved electrokinetic injection (Fig. 3). Peak amplitude increased by $53 \pm 18\%$ and more telomeric repeats could be discerned (up to 26).

Optimal injection parameters were found to be 5–8 kV and 60–300 s. Higher injection voltages (up to 10 kV) and longer injection times (up to 10 min) led to the distortion of the peaks pattern at the early (lighter) portion of a pherogram. However, the amplitude of heavier peaks continued to increase without much distortion, so these extreme injection parameters could be used to obtain a signal from much diluted samples.

In optimized CE–LIF–SPD, electropherograms of 10 cells samples exhibited pattern identical to that of negative control (i.e., early peaks of primers and 56-base red peak of internal control, and no peaks of telomeric repeats at 6-base increments), thus proving that negative PCR results for this dilution were true. This underlines the need of validation of real-time PCR results obtained for low abundance samples using such non-specific probes as SYBR Green. It also indicates that one active telomerase probably occurs in over 10 cells.

3.3. Sensitivity of telomerase detection: CE–LIF–SPD versus PCR

PCR method thus appeared to be sensitive enough to detect the minimal activity of telomerase in the experimental settings we used. These were model, ideal conditions, telomerase was extracted from cultured cells without ingress of factors that retard PCR, and, as our data suggest, PCR efficiency was close to the theoretical maximum of 2. In real clinical or forensic practice, however, samples are collected in biopsy, washout, blood, etc. They contain extracellular inhibitors of PCR, such as hemoglobin or mioglobin, as well as many non-proliferating cells, in which telomerase is suppressed by endogenous factors (Akane et al., 1994; Wu et al., 2000a). Thus, in clinical samples a variety of inhibitors may decrease PCR efficiency to below 1.5. As a result, PCR may become insufficient to amplify a diluted template to a detection threshold during 40–50 cycles. This may lead to false-negative results, missed identification of biomarkers, and missed diagnosis. These are the situations in which validation of PCR results with much more sensitive CE–LIF–SPD becomes critical.

In order to quantitatively compare sensitivities of PCR and CE–LIF–SPD, we modified our experimental model so that it emulated PCR inhibition and false-negative results. We could not achieve this by simply further diluting cell concentrations because 10 and less cell dilutions exhibit no telomerase activity. We could mix PC-3 cells with various cell populations and/or hemoglobin, but this would lessen quantification of the results and compatibility with the preceding experiments. We chose another approach: to reduce the number of PCR cycles. By this, we quantitatively mimic reduction of efficiency (hence sensitivity) of PCR and generate known false-negative samples for further CE–LIF–SPD analysis. At the same time, the rest of protocol remains unchanged. Our logic is following: if we carry out only 29 cycles of PCR, then, based on the results described above (Fig. 2), we expect PCR to detect telomerase activity only in 10^5 and 10^4 cell dilutions. 10^3 and 10^2 cell dilutions are expected to yield negative results because their fluorescence would not yet be significantly higher than background. These samples would be *known false negatives*, and they would be subjected to CE–LIF–SPD analysis. If our instrument detects telomeric repeats in 10^3 cells sample – then the sensitivity of our device would be $10^4/10^3 = 10$ times higher than that of PCR. If it detects the repeats in 10^2 cell sample – then we could claim $10^4/10^2 = 100$-fold increase in sensitivity.

3.3.1. Reduced PCR

Thus, we next conducted real-time PCR for 29 cycles. The protocol was as indicated above, except Opticon machine was stopped after 29 cycles. 10^5 cells extracts produced fluorescence significantly higher than background (Fig. 4, dashed red curve). In this particular experiment, 10^4 cells (chain orange curve) produced just under threshold level of fluorescence. It could have been considered a negative along with the solutions of lower cell concentrations (10^3: dotted green; 10^2: solid purple). Since in 40 cycles PCR the fluorescence of 10^4 cell samples crossed the threshold on average at about 28th cycle, we considered 10^4 cells as sensitivity threshold for 29 cycles PCR. Samples containing 10^3 and 10^2 cells were considered known false negatives because, even though they yielded negative results with 29 cycles PCR, we knew (see Section 3.2) that they did contain telomeric repeats.

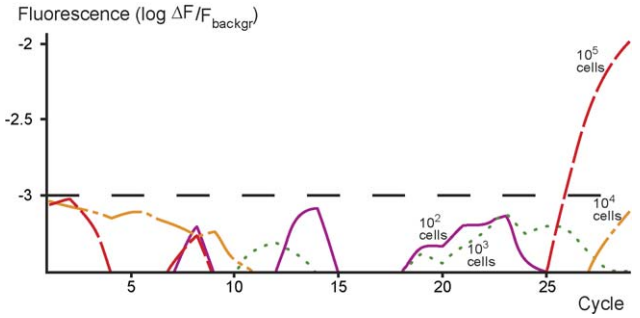

Fig. 4. Amplification during 29 cycles of real-time PCR, semi-log scale. 10^5 cells: dashed red curve; 10^4 cells: chain orange; 10^3: dotted green and 10^2: solid purple. Only 10^5 cells sample exhibited detectable amplification. Note that Fluorescence scale in this figure is about 1/10th of that in Fig. 1 or 2.

In addition, we conducted real-time PCR at further reduced number of cycles—25. No amplification was detected in any of the samples (not shown). Based on the average from 40 cycles experiments, 10^5 cells should be considered a sensitivity threshold, and 10^4, 10^3 and 10^2 cell samples—as known false-negatives for the 25 cycles PCR.

3.3.2. CE–LIF–SPD

The electropherograms of samples after 29 cycles PCR exhibited much higher fluorescence for primers and much lower for internal control and telomeric repeats as compared to corresponding cell concentrations after 40 cycles PCR. This was expected from exponential kinetics of PCR, due to which amplification occurs mainly at the later cycles. To compensate for this, we injected samples at 7 kV for 320 s, and ran CE at 10 kV. As a result, the peaks' amplitudes have increased, but so did also non-specific fluorescence of contaminants or debris, especially at lighter fractions (up to 80 bases) that include peaks of 1 through 5 repeats (Fig. 5, top trace). Therefore, we focused on examining and comparing the portions of electropherograms that start from 6-repeat peak (Fig. 5, middle trace). As demonstrated in this figure, SPD-based CE–LIF technology has revealed telomeric repeats at all cell concentrations. Characteristic repeats ladder pattern was detected even in samples with 10^2 cells extract (Fig. 5, bottom trace), which is 3 orders of magnitude lower than the lowest concentration detected in this experiment by PCR (i.e., 10^5 cells), and 2 orders of magnitude lower than average sensitivity threshold for 29 cycles PCR (i.e., 10^4 cells). Therefore, in this experiment, CE–LIF–SPD had 1000-fold higher sensitivity than real-time PCR.

Finally, we had analyzed the samples that have undergone only 25 cycles of PCR. In our instrument, telomeric repeats were detected in 10^5, 10^4, and 10^3 cells samples (Fig. 6). Desalting 10^3 cell samples and prolonging injection to 620 s had further increased the amplitude of telomeric repeat peaks (Fig. 6, bottom trace). Since no amplification was detected in this experiment by 25 cycles PCR even in 10^5 cell sample, data for the 10^5 cell extract was known false negative, and 25 cycles PCR sensitivity threshold was over 10^5. Thus, in this experiment sensitivity of CE–LIF–SPD also proved to be over 2 orders of magnitude higher than that of PCR ($>10^5/10^3 > 10^2$). On average, though,

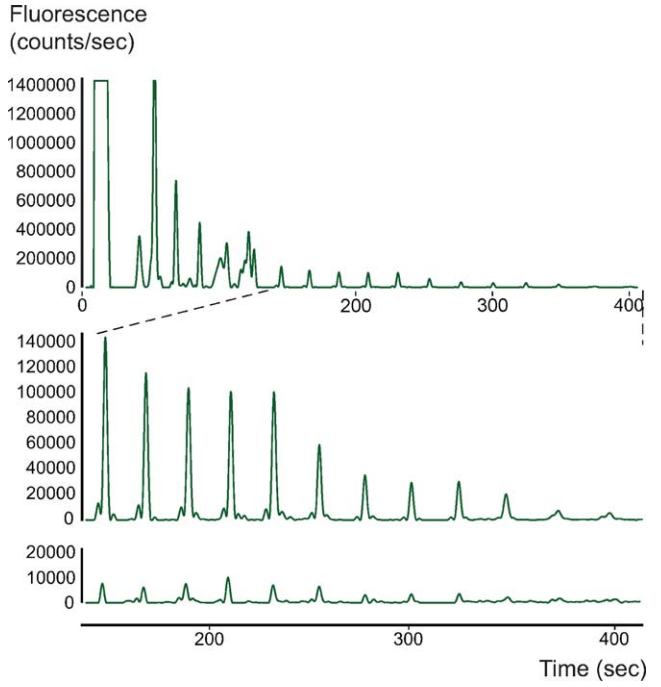

Fig. 5. Electropherograms of samples after 29 cycles PCR with TRAPeze. Top trace: extract of 10^4 cells; middle trace: expanded and amplified area of the top trace, peaks 6–17; bottom trace: expanded and amplified area of peaks 6–17 from sample with 10^2 cells extract. Traces of red-fluorescing material were omitted.

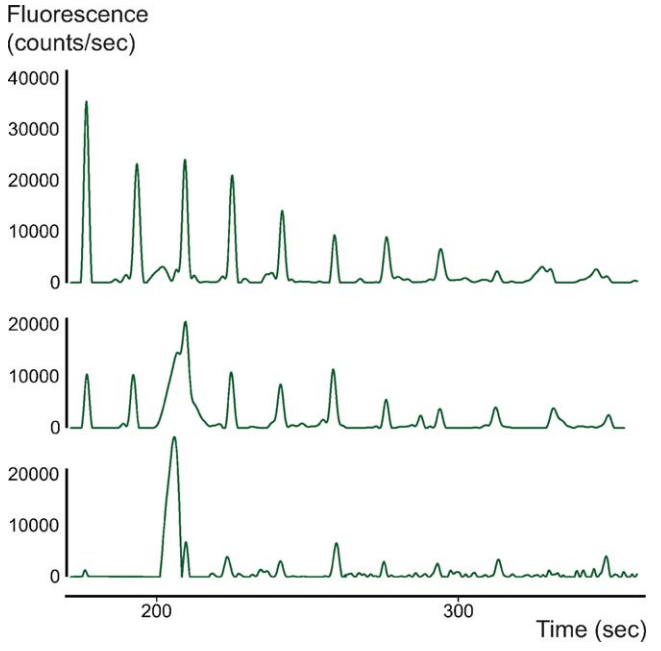

Fig. 6. Electropherograms of samples after 25 cycles PCR with TRAPeze—expanded and amplified areas of peaks 6–16. Top trace: 10^5 cells extract; middle trace: 10^4 cells; bottom trace: 10^3 cells (after desalting and 620 s electrokinetic injection). In top and middle traces, peak 8 was co-separated with debris; and in bottom trace, peaks 7 and 15 were not detected. Traces for red-fluorescing material were omitted.

CE–LIF–SPD technology again exhibited 100 times higher sensitivity than 25 cycle PCR.

4. Discussion

Using 25- and 29-cycle real-time PCR to model sub-efficient PCR in clinical samples, we have demonstrated that post-PCR fragment analysis with our SPD-based CE–LIF system yielded over 100 times higher sensitivity than most sensitive and specific real-time PCR. We believe that this ratio can be further improved by at least another order of magnitude. For example, we did not use any special signal analysis methods, whereas periodicity of telomeric repeats permits improving their signal with, for instance, auto-correlation analysis. While RTQ-TRAP detected integral signal from a ladder of amplicons, in CE their signal was divided into 10–20 peaks separated by six bases. Thus, it is reasonable to expect 10 times higher signal from single band/peak amplicons. Signal also can be improved by post-PCR clean-up of DNA, removal of primers, etc. In addition, we can optimize the instrument: use optimal filters with wider band and increase photon collection times 4-fold by using one filter instead of rotating four. Finally, there is a potential of modifying TRAPeze XL to suit real-time PCR and CE–LIF–SPD.

Although telomerase is one of potential molecular markers for cancer, there is no telomerase assay suitable for clinical testing. While PCR assays are sensitive, they have limited promise for real clinical samples because in the presence of inhibitors they yield false-negative results. Here we described the development of a highly sensitive CE–LIF–SPD-based assay for validation of telomerase activity. For the first time, we have demonstrated the use of the TRAPeze XL kit for both real-time PCR and CE–LIF; optimized PCR and CE protocols for this kit; and established that SPD-based CE–LIF has over two orders of magnitude higher sensitivity than real-time PCR with TRAPeze.

We compared PCR methods based on different chemistries – intercalating or covalently labeled probes. When combined with SYBR-based chemistry, CE did not offer any benefits over PCR. SYBR dyes are known to significantly retard and distort electrophoresis (Tuma et al., 1999), they appear to shed off DNA moving through the gel matrix and thus lose fluorescence. The advantage of covalently labeled primers is that each amplicon molecule has covalently bonded label. Although the total signal may be smaller, this benefits CE: electroseparation of fragments is more quantitative and accurate than with intercalating dyes, which bind proportionate to dsDNA length and thus cause a significant shift. In addition, covalently labeled ssDNA can be assayed with additional accuracy, and CE can be performed with a variety of advanced denaturing gel matrices.

Quality of PCR data obtained with TRAPeze was further improved by reading plate at lower temperatures where the difference between signal and background was larger. This phenomenon can be explained by the nature of Amplifluor primers: at low temperatures the hairpin loop is predominantly folded and thus energy transfer quenching within the loop is most efficient; at higher temperatures, a larger proportion of loops may stochastically open/stay open for longer times and thus allow fluorescein to emit. In PCR-extended product, however, hairpin is unfolded in dsDNA and fluoresces, but with the increase of temperature, more dsDNA molecules de-hybridize, and more hairpin structures are released and folded. At 80–85 °C, apparently all hairpin structures become single stranded and reach the same dynamic balance between folded and unfolded states as do unextended primers. This is probably why at these temperatures fluorescence of primers and amplicons becomes identical (Fig. 2). In future experiments, we plan to take plate readings at much lower temperatures, e.g., 50–55 °C.

Post-PCR fragment analysis had demonstrated that there were no telomeric repeats present in 10 and lower cell extracts. These results agree with previous reports that the TRAP-based assays have a limited linearity and reliability at concentrations lower than 250 cells (Wu et al., 2000b), and that telomerase-positive cell lines may harbor only 1 telomerase molecule per 2–6 cells (Meid et al., 2001). We excluded false-negative result with CE assay. Since TRAPeze PCR has, according to manufacturer, single-molecule resolution, the results suggest that one active telomerase may have occurred in between 10 and 100 cells. Given that we used telomerase-positive cells from cell culture lines, this suggestion may contradict the postulate that each immortal cell has an active telomerase. There could be a number of explanations. For example, only a percentage (1–10%) of an immortal population is truly immortal cells that keep proliferation and have telomerase activity. Another possibility – only a portion of the telomerase pool is active at a given point of time or cell cycle. In addition, there is a loss of enzyme during extraction of protein fraction for TRAP. All this further emphasizes the need of validation of real-time PCR results obtained for low abundance samples, and it questions usefulness in clinical practice of non-specific probes as SYBR Green.

5. Conclusions

SPD-based CE–LIF yields 100- to 1000-fold increase in the sensitivity of biomarker detection over real-time PCR. We believe that the unique sensitivity of this technology makes it especially suitable for molecular diagnostics of clinical samples, in which PCR is suppressed, may not yield a detectable signal, and may lead to missed detection and misdiagnosis of a disease. These are the situations in which ultra sensitive CE analysis of PCR products becomes critical because it enables their verification, elimination of false-positive and false-negative results, correct interpretation of the data, and thus correct patient care strategy.

Acknowledgements

This work was supported by the NIH/NCI (1R42CA10619301) and DOD, PCRP (DAMD170310020). Authors thank Mike Acosta and staff of DNA facility of the SUNY at Stony Brook for help with real-time PCR.

References

Akane, A., Matsubara, K., Nakamura, H., Takahashi, S., Kimura, K., 1994. J. Forensic Sci. 39, 362–372.

Alaverdian, L., Alaverdian, S., Bilenko, O., Bogdanov, I., Filippova, E., Gavrilov, D., Gorbovitski, B., Gouzman, M., Gudkov, G., Domratchev, S., Kosobokova, O., Lifshitz, N., Luryi, S., Ruskovoloshin, V., Stepoukhovitch, A., Tcherevishnick, M., Tyshko, G., Gorfinkel, V., 2002. Electrophoresis 23, 2804–2817.

Atha, D.H., Miller, K., Sanow, A.D., Xu, J., Hess, J.L., Wu, O.C., Wang, W., Srivastava, S., Highsmith, W.E., 2003. Electrophoresis 24, 109–114.

Blackburn, E.H., 1991. Nature 350, 569–573.

Botchkina, G.I., Kim, R.H., Botchkina, I.L., Kirshenbaum, A., Frischer, Z., Adler, H.L., 2005. Clin. Cancer Res. 11, 3243–3249.

Dhaene, K., Van Marck, E., Parwaresch, R., 2000. Virchows Arch. 437, 1–16.

Elmore, L.W., Forsythe, H.L., Ferreira-Gonzalez, A., Garrett, C.T., Clark, G.M., Holt, S.E., 2002. Diagn. Mol. Pathol. 11, 177–185.

Hess, J.L., Atha, D.H., Xu, J.F., Highsmith Jr., W.E., 2004. Electrophoresis 25, 1852–1859.

Hess, J.L., Highsmith, W.E., 2002. Clin. Chem. 48, 18–24.

Hiyama, E., Hiyama, K., 2002. Oncogene 21, 643–649.

Hou, M., Xu, D., Bjokholm, M., Gruber, A., 2001. Clin. Chem. 47, 519–524.

Jakupciak, J.P., Wang, W., Barker, P.E., Srivastava, S., Atha, D.H., 2004. J. Mol. Diagn. 6, 157–165.

Kabotyanski, E.A., Botchkina, G.I., Botchkina, I.L., Kosobokova, O., Gorfinkel, V., Gorbovitski, B., 2005. Highly sensitive measurement of telomerase activity using DNA sequencer based on single photon detection. In: Moving Biosensors to Point-of-Care Cancer Diagnostics. NIH, Maryland, pp. 25–26.

Kim, N.W., Piatyszek, M.A., Prowse, K.R., Harley, C.B., West, M.D., Ho, P.L., Coviello, G.M., Wright, W.E., Weinrich, S.L., Shay, J.W., 1994. Science 266, 2011–2015.

de Kok, J.B., Schalken, J.A., Aalders, T.W., Ruers, T.J., Willems, H.L., Swinkels, D.W., 2000. Int. J. Cancer 87, 217–220.

Meid, F.H., Gygi, C.M., Leisinger, H.J., Bosman, F.T., Benhattar, J., 2001. J. Urol. 165, 1802–1805.

Schwartz, H.E., Ulfelder, K.J., 1992. Anal. Chem. 64, 1737–1740.

Shay, J.W., Wright, W.E., 1996. Curr. Opin. Oncol. 8, 66–71.

Tuma, M.P.B., Jin, X., Jones, L.J., Cheung, C.-Y., Yue, S., Singer, V.L., 1999. Anal. Biochem. 268, 278–288.

Wege, H., Chui, M.S., Le, H.T., Tran, J.M., Zern, M.A., 2003. Nucleic Acids Res. 31, E3.

Wu, W.J., Liu, L.T., Huang, C.N., Huang, C.H., Chang, L.L., 2000a. BJU Int. 86, 213–219.

Wu, Y.Y., Hruszkewycz, A.M., Delgado, R.M., Yang, A., Vortmeyer, A.O., Moon, Y.W., Weil, R.J., Zhuang, Z.P., Remaley, A.T., 2000b. Clin. Chim. Acta 293, 199–212.